Regenerative Therapy 29 (2025) 484–492

Contents lists available at ScienceDirect

Regenerative Therapy

journal homepage: http://www.elsevier.com/locate/reth

Original Article

Exploration of the optimal retention method in vivo for stem cell therapy: Low-intensity ultrasound preconditioning

Haopeng Xu [1], Yilin Tang [1], Wenjing Mao, Liu Wu, Yiqing Zhou, Juan Deng, Wentao Tang, Xinfang Xiao, Yi Xia, Yan Wang*

State Key Laboratory of Ultrasound in Medicine and Engineering, College of Biomedical Engineering, Chongqing Medical University, Chongqing, 400016, China

ARTICLE INFO

Article history:
Received 10 January 2025
Received in revised form
26 March 2025
Accepted 17 April 2025

Keywords:
Bone marrow mesenchymal stem cells
Optimal retention method
Low-intensity ultrasound
Preconditioning
Apoptosis

ABSTRACT

Bone marrow mesenchymal stem cells (BMSCs) are pluripotent and self-renewing, exerting a crucial role in the domain of regenerative medicine. Nevertheless, BMSCs encounter challenges such as low cell viability and inadequate homing during transplantation, thereby restricting their therapeutic efficacy. Hence, current research is concentrated on identifying optimal retention approaches following BMSCs transplantation to enhance its effectiveness. Low-intensity ultrasound (LIUS) has been verified as an efficacious method to enhance the performance of BMSCs. We established a skin trauma model and assessed the therapeutic effect of LIUS-preconditioned BMSCs. The results demonstrated that pretreatment with LIUS could expedite wound healing and effectively diminish scar formation post-transplantation by promoting proliferation capacity, reinforcing anti-apoptotic attributes, improving homing ability, and significantly enhancing the transplantation effect of BMSCs. These discoveries imply that LIUS might constitute a promising strategy for attaining optimal retention after stem cell transplantation in regenerative medicine and wound repair therapy.

1. Introduction

Bone marrow mesenchymal stem cells (BMSCs), being a type of pluripotent stem cells, exhibit a high capacity for self-renewal and the potential to differentiate into multiple lineages [1]. BMSCs have been extensively explored as candidates for cell therapy [2–5], finding wide utilization in bone defect healing [6], diabetes treatment [7], and spinal cord injury management [8]. Nevertheless, during transplantation, the functional attributes of BMSCs might be impaired, resulting in suboptimal outcomes such as a low cell survival rate, insufficient cell homing, and limited stability [9]. Hence, there is an urgent requirement for a novel strategy to enhance the retention of transplanted BMSCs within target treatment areas in order to boost their therapeutic efficacy.

The LIUS is a specialized form of ultrasonic output that emits pulse waves within the frequency range of 1–3 MHz and an intensity below 1 W/cm^2 [10,11]. Recent studies have demonstrated the significant impact of LIUS on the biological activity of BMSCs by promoting their proliferation, differentiation, and migration [12–15]. However, there have been no reports on whether LIUS improves the optimal retention method of BMSCs in vivo.

Therefore, in order to validate the potential of LIUS in enhancing the homing ability, activity, and stability of BMSCs in vivo, we have designed the following experimental protocol: establishing a skin trauma model and subsequently transplanting LIUS-preconditioning BMSCs into the wound site. This approach aims to evaluate whether this intervention can enhance the efficacy of stem cell transplantation and determine its potential as an optimal method for stem cell retention.

Abbreviations: BMSCs, Bone marrow mesenchymal stem cells; LIUS, Low-intensity ultrasound; SD, Sprague dawley; DMEM, Dulbecco's modified eagle medium; MTT, Methyl thiazolyl tetrazolium; PBS, Phosphate buffered saline; DEGs, Differentially expressed genes; H&E, Hematoxylin and eosin; ELISA, Enzyme-linked immunosorbent assay; PDGF, Platelet-derived growth factor; TNF-α, Tumor necrosis factor-α; SDF-1, Stromal cell-derived factor-1; ECM, Extracellular matrix.

* Corresponding author. State Key Laboratory of Ultrasound in Medicine and Engineering, College of Biomedical Engineering, Chongqing Medical University, 1 Yixueyuan Rd, Yuzhong District, Chongqing, China.

E-mail address: wangyancq@cqmu.edu.cn (Y. Wang).

Peer review under responsibility of the Japanese Society for Regenerative Medicine.

[1] Haopeng Xu and Yilin Tang are contributed equally to this work and shall share first authorship.

https://doi.org/10.1016/j.reth.2025.04.012

2. Materials and methods

2.1. In vitro experiments

2.1.1. Cell culture

The BMSCs of Sprague Dawley (SD) rats were obtained from Saiye Biological Co., Ltd (Product number: RASMX-01001). The cells were cultured in a humidity-saturated incubator at 37 °C with 5 % CO_2 using low-glucose Dulbecco's modified Eagle's medium (DMEM) supplemented with 10 % fetal bovine serum and 1 % penicillin-streptomycin.

The BMSCs, which had undergone three generations of passage, were seeded into 96-well plates at a density of 4×10^3 cells per well. Two groups were established: the LIUS group and the Control group, each consisting of six replicate wells and blank wells. In the LIUS group, BMSCs were exposed to LIUS for 20 min daily over a period of seven days. The parameters used for LIUS treatment were as follows: sound intensity of 30 mW/cm^2, frequency of 0.3 MHz, repetition rate of 1 kHz, and duty cycle of 20 % [16]. In the Control group, BMSCs received no energy output during LIUS exposure.

2.1.2. Cell viability assay

After a 6-h interval following the termination of LIUS irradiation on the 7th day, the Methyl Thiazolyl Tetrazolium (MTT) assay was conducted using MTT powder (Solarbio Technology Co., Ltd, Beijing) in accordance with the manufacturer's instructions. Subsequently, absorbance at 490 nm was measured utilizing an automatic microplate reader (TECAN Co., Switzerland).

2.1.3. Fluorescence staining

After 7 days of irradiation, the BMSCs in both the LIUS group and Control group were fluorescently labeled with PI/DAPI and JC-1 to observe apoptosis and changes in mitochondrial membrane potential. Subsequently, the results were observed under a fluorescence microscope (Olympus Co., Canada).

2.1.4. Flow cytometry detection

After 7 days of irradiation, the suspended cells were obtained through routine trypsin digestion and centrifugation (Hyclone Co., USA). Subsequently, the cells were washed with Phosphate Buffered Saline (PBS, Hyclone Co., USA). The apoptosis rate of BMSCs was assessed using Annexin V/PI double staining, while the calcium ion concentration was measured by Fluo-3 fluorescent labeling. Both assessments were conducted using flow cytometry (Beckman Co., USA), following the manufacturer's instructions.

2.1.5. RNA-seq and bioinformatic data analysis

After 7 days of irradiation, BMSCs from the LIUS group and Control group were collected for subsequent RNA sample processing and RNA-seq analysis conducted by Shenzhen BGI Co., Ltd. DESeq2 software was employed to analyze gene differences, with log2 (Fold Change) >1 and $P < 0.05$ serving as the criteria to identify differentially expressed genes (DEGs).

2.2. In vivo experiment

2.2.1. Animals

The SD rats, all female and aged 8–10 weeks, were sourced from the Experimental Animal Center of Chongqing Medical University. All rats were maintained under controlled conditions with a temperature of 25 °C, humidity of 45 %, and a light cycle of 12 h per day. The project strictly adhered to the ethical standards set by the Experimental Animal Ethics Committee of Chongqing Medical University. Experiments were conducted in compliance with national and institutional guidelines for animal care and use, authorized by Chongqing Medical University's ethics board (approval number: 2022099).

2.2.2. Wound healing model building

The SD rats were anesthetized by intraperitoneal injection of 10 % pentobarbital sodium (35 mg/kg body weight). Subsequently, the dorsal skin was depilated and disinfected with 75 % alcohol (Chengdu Kelong Chemical Reagent factory, Sichuan, China) three times. Utilizing sterile ophthalmic scissors, the epidermis and dermis of the dorsal skin were excised to create a circular model of total skin injury with a diameter of 2 cm [7]. Upon completion of the modeling process, the rats were housed in individually ventilated cages.

2.2.3. Group and treatment

The successfully modeled SD rats were divided into five groups (n = 30) as follows.

- LIUS group: Apply ultrasound coupling agent around the skin lesion on the back of the rat, placing the probe on the skin coated with the coupling agent (avoiding irradiation of the lesion area). The parameters of LIUS used were as follows: sound intensity of 200 mW/cm^2, frequency of 0.3 MHz, repetition frequency of 1 KHz, duty cycle of 20 %, once a day for a duration of 20 min over a period of 7 days. Additionally, 1 ml of physiological saline was injected 0.5 cm around the incision.
- BMSCs group: Rats received an equal amount of 1 ml BMSCs suspension (1×10^6/mL) around the incision site and no energy output from the probe was applied to irradiate the skin lesion.
- LIUS + BMSCs group: Similar to the BMSCs group, rats received an injection of BMSCs suspension and also underwent LIUS irradiation as described in the LIUS group.
- LIUS + PC-BMSCs group: In this group, BMSCs were preconditioned with LIUS using parameters such as sound intensity at 30 mW/cm^2, frequency at 0.3 MHz, repetition frequency at 1 KHz, and duty cycle at 20 %. This preconditioning was performed once a day for a duration of 20 min over a period of seven days. Subsequently, rats received an injection of preconditioned BMSCs suspension (1×10^6/mL) around the skin lesion.
- Control group: Rats in this group received an same volume of 1 ml physiological saline injection around the skin lesion, and sham irradiation was performed at the same time.

The flow chart depicting these experimental procedures is shown in Fig. 1.

2.2.4. Immunofluorescence

To assess the in vivo viability of BMSCs, immunofluorescence was performed to detect the expression of CD90 protein on BMSCs. Skin samples collected at 1d and 3d were processed for paraffin sectioning (section thickness: 3.5 μm). The sections were then routinely dewaxed, dehydrated, antigen-repaired, and blocked before being incubated with primary antibody against CD90 (DF4804, Affinity, Jiangsu, China), followed by secondary antibodies (S0008, Goat Anti-Rabbit lgG (H + L) FITC-conjugated, Affinity, Jiangsu, China) and DAPI staining (D1306 Invitrogen USA). Finally, the sections were observed under a Nikon inverted fluorescence microscope (Model TE-2000U; Nikon Tokyo Japan).

2.2.5. Wound healing rate

The wound condition and complete healing time were recorded for each group of rats on days 0, 3, 7, 14, and 28. Subsequently, the data was analyzed using Image J (NIH, Bethesda, MD). The wound

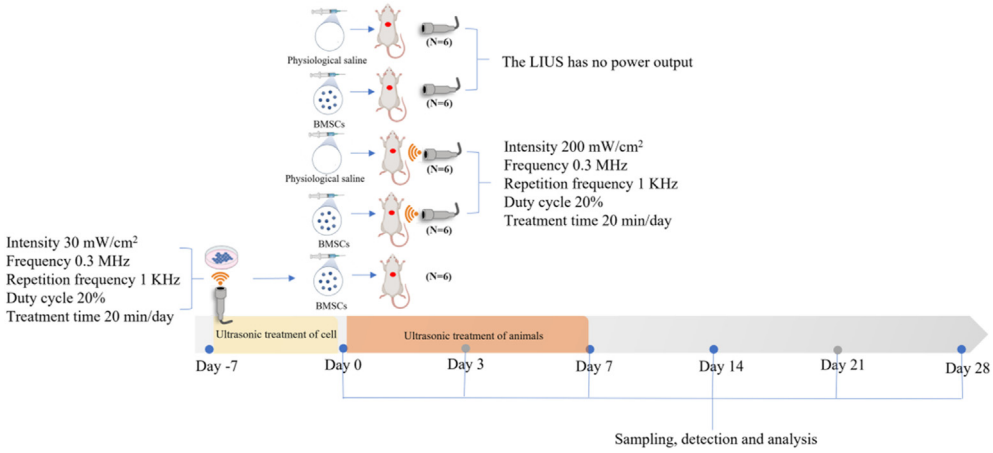

Fig. 1. The flow chart of the in vivo experiment.

healing rate was calculated as [(initial wound area - current wound area)/initial wound area] × 100 %.

2.2.6. Hematoxylin and eosin (H&E) staining

The skin lesion tissue slices from each group were dewaxed for H&E staining, followed by visualization using an optical microscope (BX51, Olympus, Tokyo, Japan) and analysis using Image J.

2.3. Masson staining

The skin samples collected on day 28 were subjected to Masson staining using a Masson staining kit (Solebao Technology Co., Ltd, Beijing, China). Subsequently, the collagen fibers in each group were evaluated using an optical microscope and Image J software.

2.3.1. TUNEL assay

Apoptosis in the lesion area was detected using the TUNEL apoptosis assay kit (Beyotime Biotechnology Co., Ltd, Shanghai, China) in accordance with the manufacturer's instructions and observed under a fluorescence microscope.

2.3.2. Immunohistochemistry

To assess the status of macrophages, endothelial cells, and apoptosis-related proteins, immunohistochemical analysis was performed to detect the expression levels of Bax (AF0120, Affinity, Jiangsu, China), Bcl2 (AF6139, Affinity, Jiangsu, China), and Caspase-3 (AF6311,Affinity, Jiangsu,China) with a dilution ratio of 1:50–1:200. Five random visual fields were selected under an optical microscope for analysis using Image J.

2.3.3. Quantitative real-time PCR (qRT-PCR)

To assess the expression of Bax and Bcl-2 related mRNA during the proliferative phase of wound healing, total RNA was extracted from the tissue of skin lesions at 7d and subsequently reverse transcribed into cDNA. The experiment was conducted using a fluorescence quantitative PCR instrument (Bio-rad Co, US), and data analysis was performed using the $2^{-\triangle\triangle}$ CT method. The primer is as follows:

Bax-F: GGCGATGAACTGGACAACAACA.
Bax-R: GCTGCCACACGGAAGAAGAC.
Bcl-2-F: TCTTCAGAGACAGCCAGGAGAA.
Bcl-2-R: GTGTGGAGAGCGTCAACAGG.

2.3.4. Toluidine blue staining

The slides were subjected to dewaxing, hydration, and toluidine blue staining in order to investigate mast cell changes during wound inflammation. Subsequent observations were made under an optical microscope.

2.3.5. Enzyme-linked immunosorbent assay (ELISA)

The levels of platelet-derived growth factor (PDGF), tumor necrosis factor-α (TNF-α), and stromal cell-derived factor-1 (SDF-1) in skin tissue were quantified using ELISA kits provided by Jingmei Biotechnology Co., Ltd. located in Jiangsu, China.

2.4. Statistical analysis

The experiments were repeated a minimum of three times to ensure the study's reliability. Data analysis was performed using GraphPad Prism Version 8 software (GraphPad Software Inc., San Diego, CA) and presented as means ± standard deviation. Each experiment was conducted in triplicate. Statistical differences were assessed using T-test, one-way ANOVA, or two-way ANOVA. A significance level of $P < 0.05$ indicated statistical significance, while $P < 0.01$ denoted high significance ($^{*}P < 0.05$, $^{**}P < 0.01$).

3. Results

3.1. The efficacy of stem cell transplantation has been enhanced and its therapeutic potential has been optimized

As shown in Fig. 2A and B, transplantation of LIUS-preconditioned BMSCs significantly enhanced wound healing compared to the untreated group. The wound healing rate in the LIUS + PC-BMSCs group was notably higher than that in other groups on both the 3rd and 14th day, resulting in a significant reduction in healing time ($P < 0.05$). Remarkably, we observed that the LIUS + PC-BMSCs group exhibited the smallest scar area after LIUS preconditioning (Fig. 2C). These findings suggest that LIUS preconditioning improves BMSC proliferation and homing ability, leading to remarkable efficacy in promoting wound healing and reducing scarring.

The histopathological examination of the skin sections disclosed a considerable presence of inflammatory cells, neovascularization, and fibroblasts in all experimental groups on day 3. Additionally, H&E staining manifested the gradual establishment of granulation tissue. By day 7, the granulation tissues in all groups demonstrated

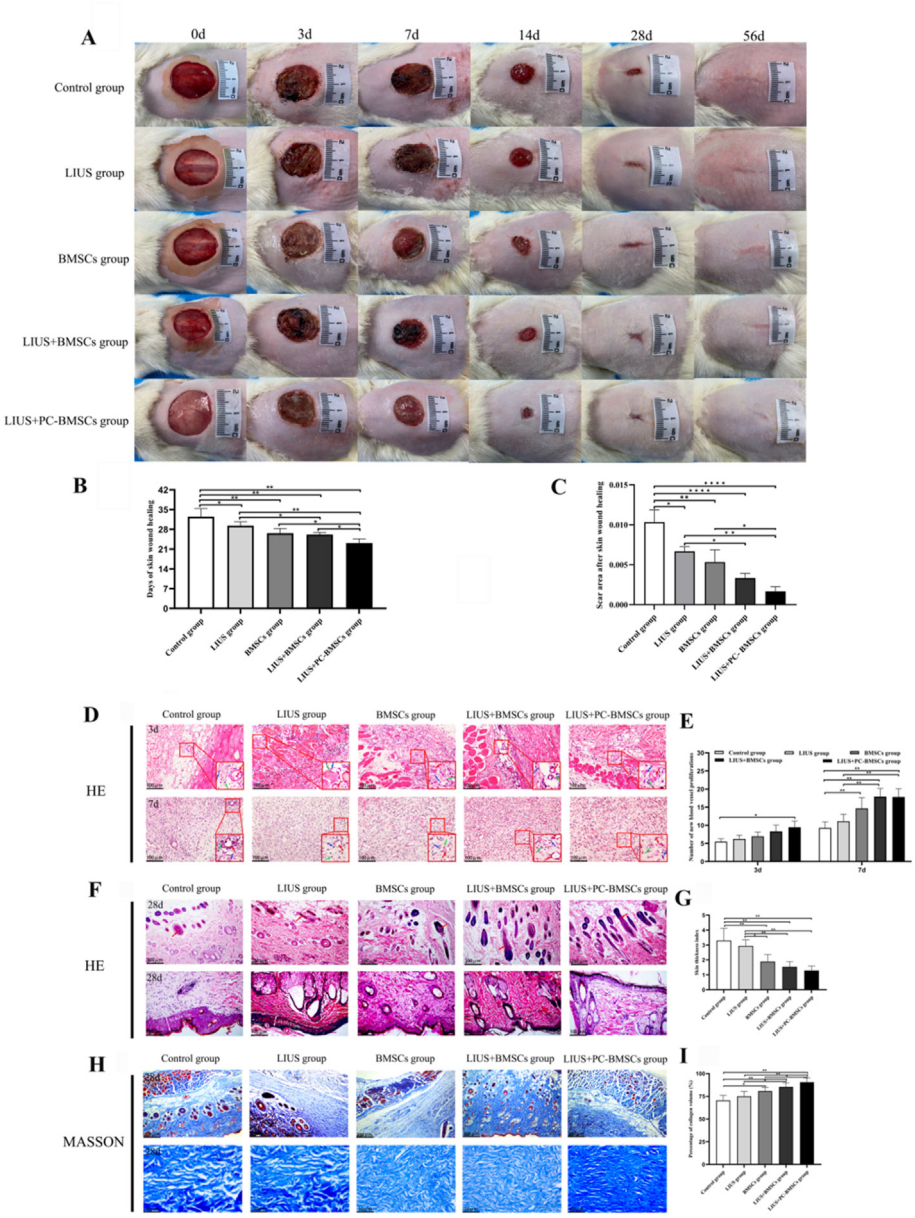

Fig. 2. A. The healing of skin wounds in each group of rats. B. The days of skin wound healing in each group. C. Scar area after skin wound healing in each group. D. The H&E staining of skin lesions in inflammatory and proliferative phases in each group (×100, ×200). E. Comparison of the amount of neovascularization in inflammatory and proliferative phases of skin lesions in each group. F. The H&E staining of skin lesions in the remodeling phase in each group (×100, ×200). G. Comparison of epidermal thickness index in remodeling phase of skin lesions in each group. H. The Masson staining of skin lesions in the remodeling phase in each group (×100, ×400). I. Comparison of percentage of collagen volume in the remodeling stage of skin lesions in each group. *$P < 0.05$; **$P < 0.01$.

augmented growth and maturation, along with an increase in neovascularization. Notably, the LIUS + PC-BMSCs group exhibited a significantly higher quantity of new blood vessels ($P < 0.05$) in comparison to other groups (Fig. 2D and E). On day 28, there was a reduction in the composition of granulation tissue across all groups; however, the LIUS + PC-BMSCs group presented the most remarkable degree of differentiation with a notable increment in hair follicles (Fig. 2F). The analysis of the epidermal thickness index (epidermal thickness index=[average epidermal thickness within lesion area/average normal skin thickness]) indicated that the ratio for the LIUS + PC-BMSCs group was closest to 1, suggesting that its epidermis closely resembled normal skin tissue (Fig. 2G).

Additionally, Masson staining revealed that by day 28, the skin wounds in each group had essentially healed and collagen deposition had commenced. In the control group, some areas exhibited loose and thin collagen fibers, whereas the majority of collagen fibers in the LIUS + PC-BMSCs group appeared dense and robust (Fig. 2H). The percentage of collagen volume was significantly higher in the LIUS + PC-BMSCs group compared to the Control group ($P < 0.01$), and there was a statistically significant difference in collagen deposition between the LIUS + PC-BMSCs group and BMSCs group ($P < 0.05$) (Fig. 2I). These findings demonstrate that the LIUS + PC-BMSCs group exhibited superior skin repair quality.

3.2. The efficacy of stem cell transplantation has been enhanced and its retention technique has been optimized

In vitro experiments revealed that LIUS preconditioning of BMSCs enhanced their proliferative activity and reduced the rate of apoptosis (Fig. 3A and B). Compared to the control group, LIUS

preconditioning of BMSCs significantly decreased the number of late apoptotic cells ($P < 0.05$) (Fig. 3C). The decline in mitochondrial membrane potential is a key indicator of early apoptosis. Fluorescence microscopy demonstrated that the LIUS + PC-BMSCs group exhibited the least decrease in mitochondrial membrane potential (Fig. 3D and E). Cell apoptosis and proliferation are closely associated with intracellular calcium concentration. Fluo-3f fluorescence staining indicated that LIUS preconditioning increased intracellular calcium concentration in BMSCs ($P < 0.05$) (Fig. 3F). These findings suggest that LIUS preconditioning can effectively reduce early apoptosis in BMSCs.

The TUNEL staining technique was employed to further validate in vivo that LIUS preconditioning of BMSCs resulted in a reduction in the apoptosis rate of cells associated with skin lesions. On day 7, the apoptosis index of the LIUS + PC-BMSCs group exhibited a significantly lower value compared to other groups (Fig. 4A and B). To explore the mechanism by which BMSCs regulated apoptosis in the proliferative phase after LIUS preconditioning, we performed immunohistochemical staining for Caspase-3, Bax and Bcl-2 in tissue sections of the skin lesions at 7 days in each group.These findings demonstrated that Bcl-2 protein was strongly positive, Bax protein and Caspase-3 protein were weakly positive in LIUS + PC-BMSCs group, which was just opposite in the Control group (Fig. 4C–H). This suggests that LIUS preconditioning of BMSCs can mitigate apoptosis during the proliferative stage of skin lesions through modulation of the Bcl-2 apoptotic pathway. Similar results were obtained using qPCR analysis. Compared to the control group, mRNA expression related to Bax was down-regulated and mRNA expression related to Bcl-2 was up-regulated in all other groups; however, these changes were most significant in the LIUS + PC-BMSCs group ($P < 0.05$) (Fig. 4I and J). ELISA measurements revealed serum levels of PDGF and TNF-α. The results indicated that LIUS preconditioning of BMSCs could enhance secretion levels of PDGF and TNF-α during both inflammatory and proliferative phases. Throughout wound healing, there was an initial increase followed by a subsequent decrease in TNF-α and PDGF contents ($P < 0.05$) (Fig. 4K-L). Collectively, these findings suggest that the antiapoptotic capability conferred by LIUS preconditioning on BMSCs may be attributed to its ability to attenuate inflammatory responses.

CD90 is a crucial marker protein for the homing of BMSCs. The results demonstrated that the expression rate of CD90 positivity in skin sections of SD rats was highest in the LIUS + PC-BMSCs group (Fig. 5A and B). Furthermore, the homing ability of the LIUS + PC-BMSCs group was significantly superior to that of other groups. It has been reported that SDF-1 plays a pivotal role in cell activation during BMSCs homing [17]. ELISA analysis revealed that LIUS preconditioning could enhance SDF-1 secretion during both inflammatory and proliferative stages ($P < 0.05$) (Fig. 5C).

Long-term in vitro culture of BMSCs may induce heterogeneity, potentially compromising the stability of these cells. On the 7th day of in vitro culture, both the control group and LIUS group exhibited spindle-shaped or triangular BMSCs that were uniform, dense, and displayed robust growth (Fig. 5D). These findings suggest that LIUS preconditioning does not alter the morphology of BMSCs. Furthermore, histological analysis using H&E staining (Fig. 2D) revealed distinct tissue boundaries with increased presence of inflammatory cells, neovascularization, fibroblasts, and progressive formation of granulation tissue without any evidence of tumor infiltration or abnormal cellular changes. Collectively, these results demonstrate that transplantation of LIUS preconditioned BMSCs can effectively promote skin repair in vivo while maintaining their inherent stability.

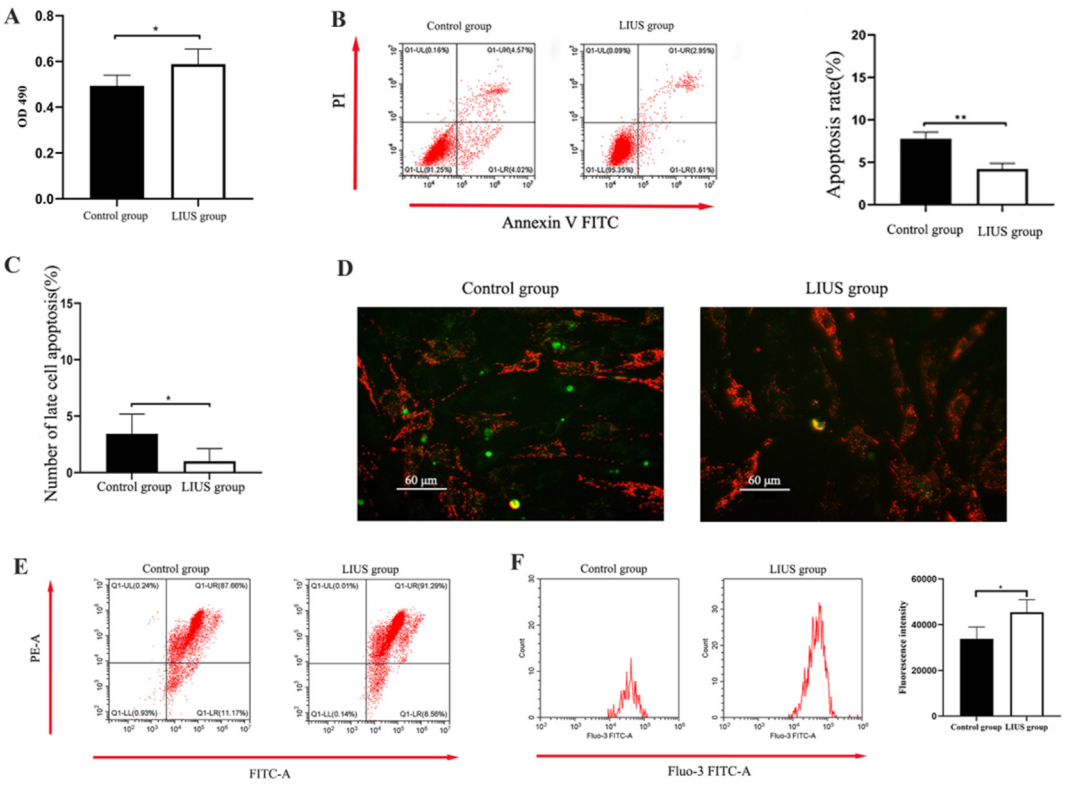

Fig. 3. A. The proliferative activity of BMSCs was detected by MTT. B. The effect of LIUS on the apoptosis rate of BMSCs was detected by flow cytometry. C–D. Detection of the mitochondrial membrane potential of BMSCs in each group by JC-1 staining (×200). E–F. Fluo-3 fluorescent staining was used to detect the intracellular calcium concentration in the LIUS group and Control group. *$P < 0.05$; **$P < 0.01$.

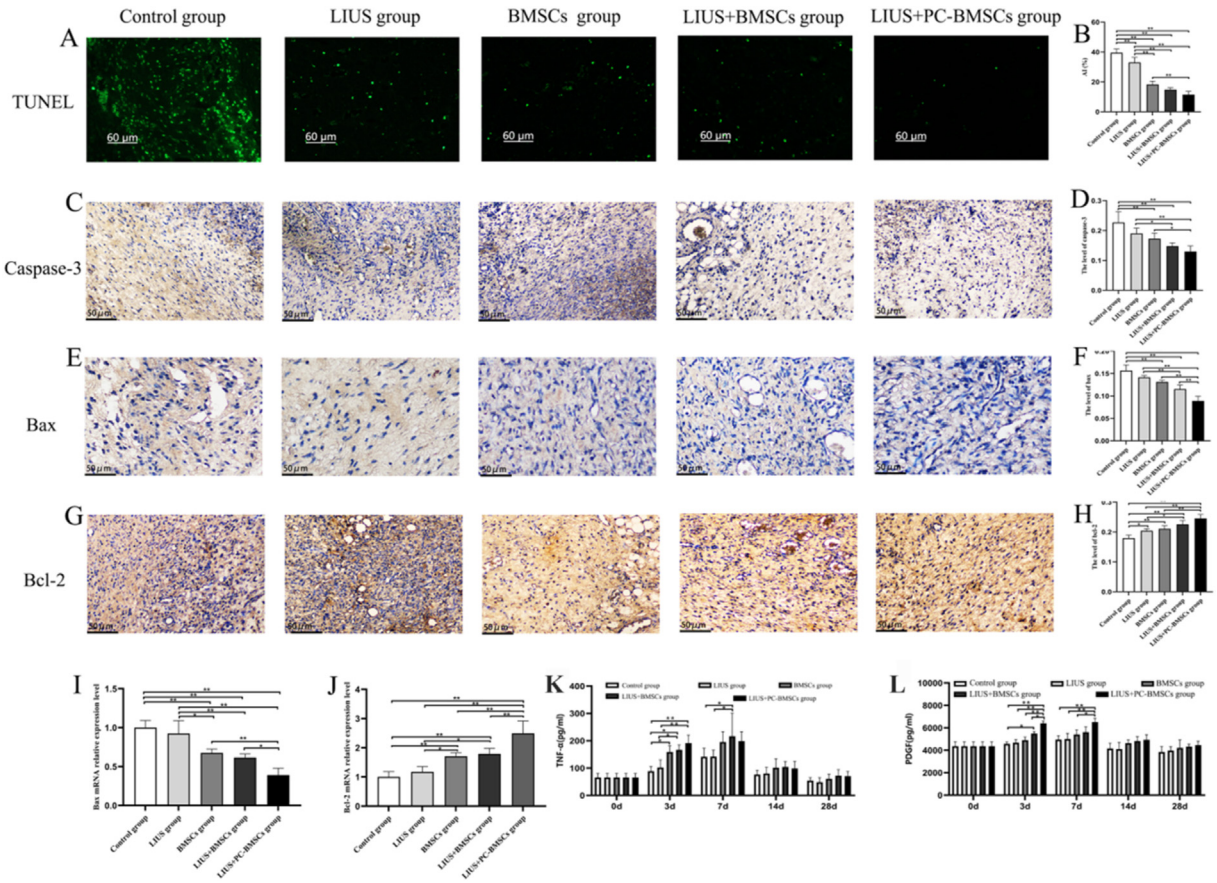

Fig. 4. A. The TUNEL detection of apoptosis of skin lesions in the proliferative phase in each group (×400). B. Comparison of apoptosis index in each group. C–H. Immunohistochemical detection of Caspase-3, Bax, and Bcl-2 expression of skin lesions in the proliferative phase in each group (×400). I–J. Comparison of relative expression of Bax and Bcl-2-related mRNA in the proliferative phase of skin lesions in each group. K–L. Comparison of serum TNF-α and PDGF levels in each group. *$P < 0.05$; **$P < 0.01$.

3.3. The impact of LIUS preconditioning on the gene expression of BMSCs

To investigate the impact of LIUS on gene expression in BMSCs, we conducted a transcriptome RNA-seq analysis. After screening 83 differentially expressed genes (DEGs), we identified 31 up-regulated DEGs and 52 down-regulated DEGs. Notably, Rfxap, RELN, LILRB3A, BDKRB2, CACNA1I, ATP13A4, Ston2, ID1, SACS and Katnall exhibited the most significant up-regulation while Tsr2, Alpl, Npr3, Cpz, Pln, Agtr2, Adamts9, Lmcd1, Cxcl13 and Nrxn2 showed the most significant down-regulation. Analysis of the volcano plot of DEGs (Fig. 6A) and clustering heat map of DEGs (Fig. 6B) revealed that these genes primarily influenced cell proliferation; development of extracellular matrix (ECM) tissue; differentiation of neurons and skeletal muscle cells; aggregation of cartilage; intracellular calcium ion concentration; as well as activity of multiple growth factors and their receptors. The GO enrichment analysis (Fig. 6C) and KEGG enrichment analysis (Fig. 6D) of differential genes revealed that the differentially expressed genes primarily impacted three key pathways: the calcium signaling pathway (upregulation of Bdkb2, Cacna1i, and Itpr3 genes; downregulation of Pln, Adrb3, Tbxa2r, F2R, and Avpr1a genes), signaling pathways controlling stem cell pluripotency (upregulation of Id1, Id2, and Id3 genes; downregulation of Fzd4 and Pik3r3 genes), and Hippo signaling pathway (upregulation of Id1 and Id2 genes; downregulating Tgfb2, Fzd4, and Ccn2 genes).

4. Discussion

BMSCs hold immense promise in regenerative medicine; however, their therapeutic potential is frequently constrained by suboptimal retention approaches in cell therapy. In this study, we employed LIUS to precondition BMSCs with the objective of augmenting their biological activity. Our findings indicated that LIUS preconditioning conspicuously enhanced the proliferative capacity, anti-apoptotic characteristics, stability, and chemotactic homing capabilities of BMSCs. Significantly, LIUS-preconditioned BMSCs expedited wound healing and mitigated scar formation after transplantation, thereby considerably enhancing the efficacy of BMSC transplantation.

The transition of BMSCs from a stable and controlled in vitro environment to a variable and challenging in vivo setting may compromise their survival rates, homing characteristics, and overall stability, factors that contribute to reduced transplantation efficiency [18].

The previous studies have demonstrated that exogenous BMSCs utilized for tissue regeneration often encounter the challenge of a high apoptosis rate following transplantation [19]. Therefore, it is crucial to investigate an optimal retention method for BMSCs in order to enhance their transplantation outcomes. Our findings revealed that LIUS preconditioning not only augmented cellular activity but also significantly fortified the anti-apoptotic capacity of these cells.

Our investigation revealed that compared to the control group, the LIUS group also demonstrated enhanced wound healing.

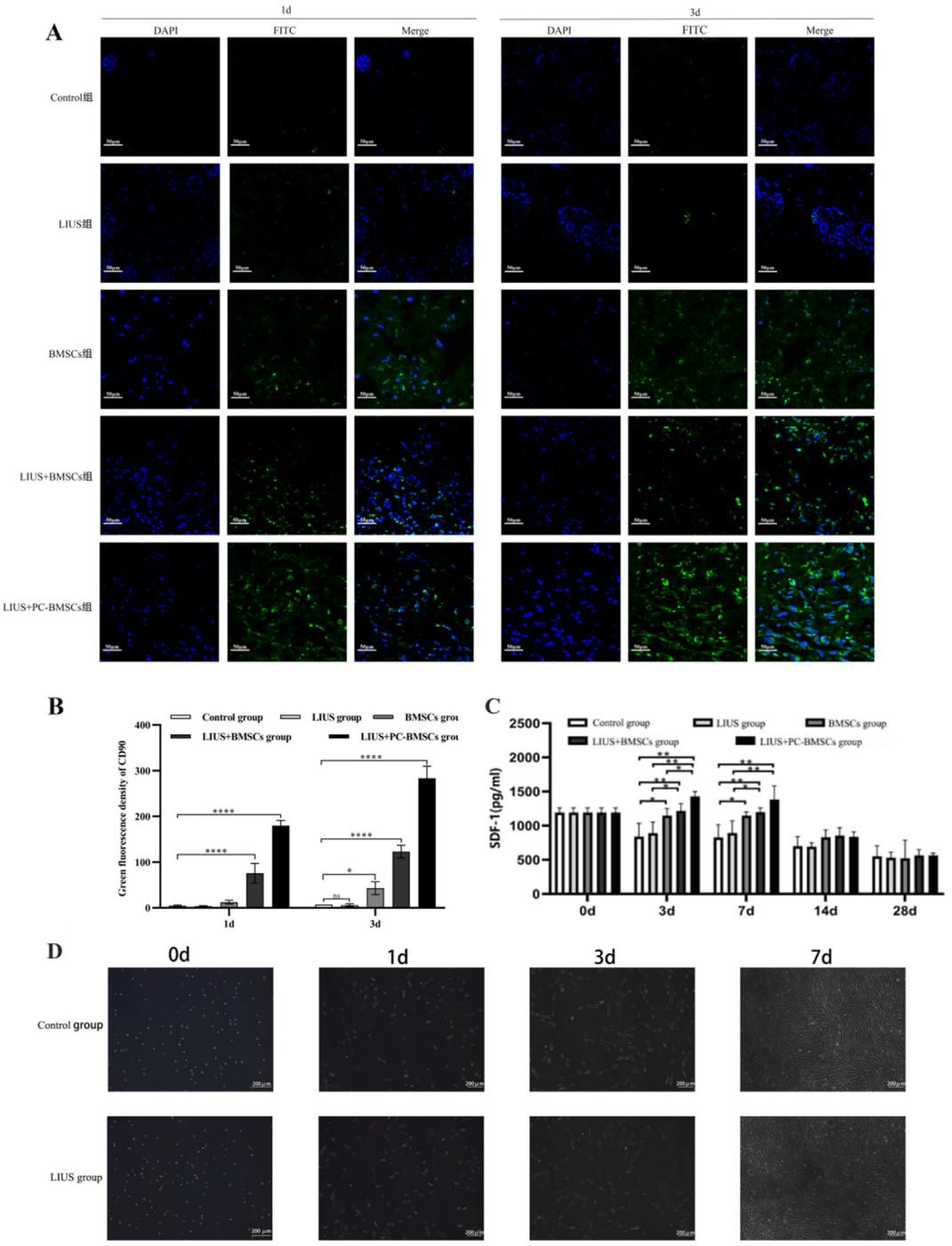

Fig. 5. A. Fluorescent CD90 labelling of BMSCs and distribution in skin tissues in each group. B. Green fluorescence density of CD90 in each group. C. Comparison of serum SDF-1 levels in each group. D. The morphology of BMSCs after LIUS irradiation was observed under optical microscope (×40). *$P < 0.05$; **$P < 0.01$; ****$P < 0.0001$.

Wakabayashi et al. revealed that low-frequency ultrasound facilitates wound repair, correlating with early-stage neovascularization and later-phase increases in collagen matrix production and epithelialization [20]. While our experimental results indicate that the group with LIUS + PC-BMSCs group showed the best effects in accelerating wound healing and reducing scar formation after transplantation. LIUS treatment effectively enhanced the proliferation of BMSCs, which is consistent with previous experimental findings reported by Yang et al. [21] and Xie et al. [22]. CD90 serves as a crucial marker for evaluating the homing ability of BMSCs [23]. Through immunofluorescence analysis, we observed that the LIUS + PC-BMSC group exhibited the highest rate of positive CD90 expression following LIUS preconditioning. Additionally, SDF-1 plays a crucial role in activating cells during the homing process of BMSCs [17]. Previous studies have indicated that LIUS can enhance migration through autophagy-regulated signaling pathways involving SDF-1 [24]. Our research further demonstrates that transplantation of LIUS preconditioned BMSCs leads to significantly increased secretion levels of SDF-1 during both inflammatory and proliferative phases. This suggests that LIUS preconditioning may

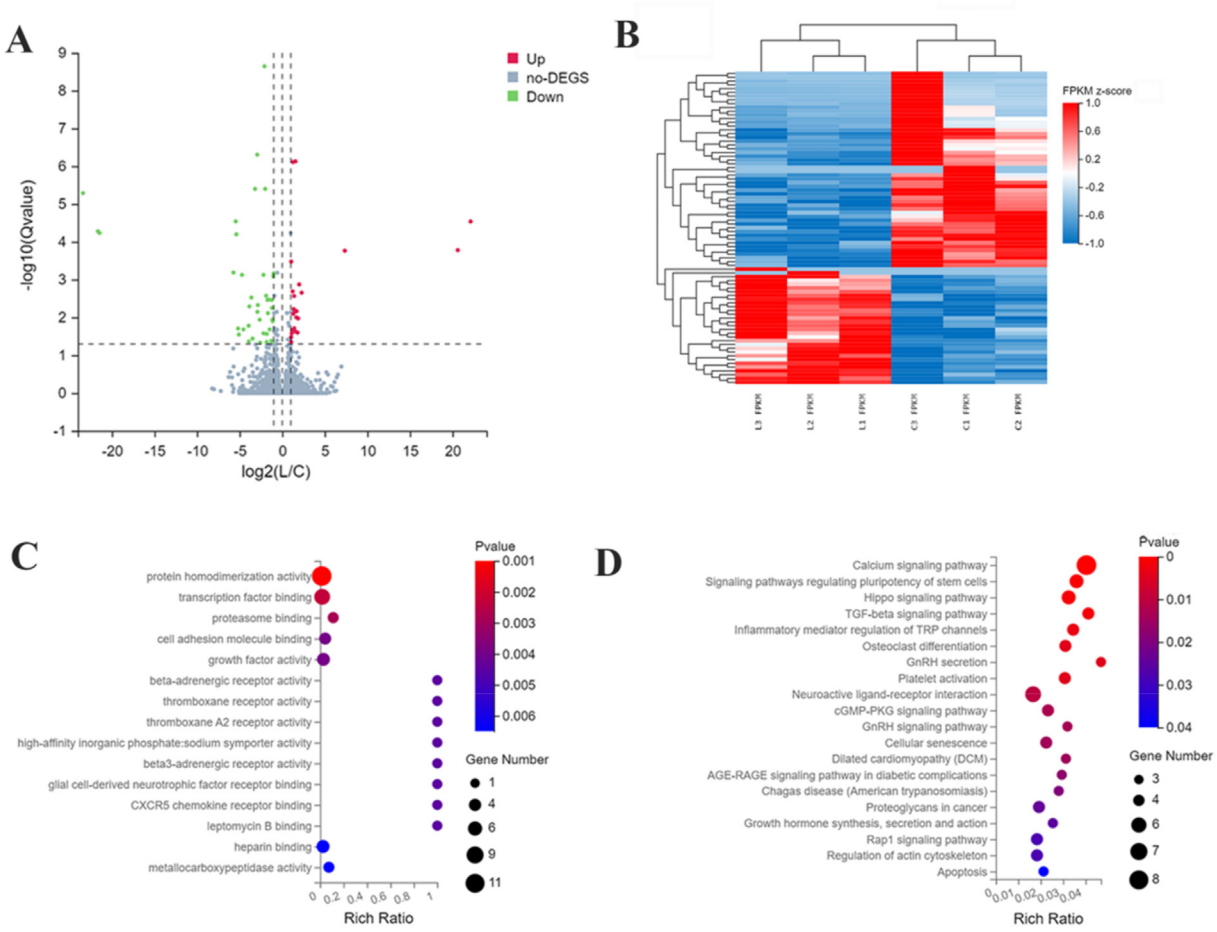

Fig. 6. A. The volcano map of DEGs. B. The clustering heat map of DEGs. C. The GO enrichment analysis (biological process) of DEGs. D. The KEGG enrichment analysis of the DEGs.

optimize the homing capability of BMSCs by modulating the secretion levels of SDF-1.

It is worth noting that while the combination of self-renewal capabilities and continuous proliferation endows BMSCs with significant therapeutic potential [25], they may also exhibit growth patterns resembling tumor cells, particularly in long-term cultured stem cells [26]. This could result in heterogeneity issues affecting stability and directed migratory abilities, thereby impacting both transplantation efficiency and tissue regeneration outcomes. However, morphological assessments indicated no structural alterations in BMSCs resulting from LIUS pretreatment. Furthermore, histological examination using H&E staining revealed the presence of numerous inflammatory cells alongside neovascularization and fibroblasts across all groups' skin sections. Granulation tissue formation was observed without any signs indicative of tumor infiltration or abnormal cellularity. These findings suggest that transplantations involving LIUS preconditioning of BMSCs promote effective skin repair processes without the risk of malignant transformation, thus affirmatively highlighting the beneficial role played by such treatments in maintaining stability within transplanted populations.

To further elucidate the mechanisms underlying the enhancement of outcomes associated with BMSCs transplants by LIUS, we employed RNA sequencing technology. This revealed an upregulation of Id1 expression and a suppression of Tsr2 expression following treatment application. Previous literature suggests that increased expressions of Id1 and Id2 genes are positively correlated with enhanced cellular anti-apoptotic functionalities [27–29]. In this study, the up-regulation of Id1 expression after ultrasonic preconditioning may be one mechanism through which LIUS enhances the anti-apoptotic activity of BMSCs.

The influence of LIUS on the viability, proliferation, differentiation, and migration aspects of BMSCs functionality through mechanical stimulation has been substantiated by existing investigations, different LIUS parameters have different effects on BMSCs [30–33]. However, further studies are needed to explore the effect of LIUS preconditioning on the differentiation ability of BMSCs. Additionally, considering the inherent heterogeneities among individual derived sources and their distinct attributes tied directly back into respective tissues, personalized approaches tailored accordingly will be necessary to ensure efficient implantation. These multifaceted considerations call for future explorations aimed at validation.

5. Conclusion

In conclusion, LIUS preconditioning emerges as a novel and promising therapeutic strategy to enhance the retention and efficacy of BMSCs in regenerative medicine and wound repair. This approach not only stimulates proliferation and augments anti-apoptotic properties of BMSCs but also enhances their homing capacity and maintains their stability, thereby substantially improving the outcomes of BMSCs transplantation. While our findings are promising, it is important to note that further studies are needed to fully elucidate LIUS preconditioning enhances the mechanisms associated with optimal retention in BMSCs transplantation.

Author contributions

YW conceived and designed the experiment, while HX and YT conducted the experiment and completed the manuscript with assistance from WM, LW, and YZ. JD, WT, XX, and YX performed the detection of experimental indicators. HX, YT, and YW analyzed and processed the data. The final manuscript was reviewed and approved by all authors.

Availability of data and materials

The datasets used and/or analyzed during the current study are available from the corresponding author on reasonable request. This paper did not generate new unique reagents.

Ethics approval and consent to participate

The study was approved by the Ethics Committee of the Animal Experiment Center of Chongqing Medical University on September 9, 2022, with approval number 2022099. The animal study further conforms to the Animals in Research: Reporting In Vivo Experiments (ARRIVE 2.0) guidelines, which provide a comprehensive framework for reporting animal research to enhance transparency and reproducibility. The experimental procedures adhered to the principles outlined by the International Council for Laboratory Animal Science (ICLAS), following the ethical principles of rational use of experimental animals to ensure the welfare of experimental animals.

Consent for publication

Not applicable.

Funding

This research was partially supported by the Program for Youth Innovation in Future Medicine, Chongqing Medical University [Number: W0155].

Declaration of competing interest

The authors declare that they have no known competing financial interests or personal relationships that could have appeared to influence the work reported in this paper.

Acknowledgments

We thank J. Xu for his assistance in the preparation of the slices and H&E staining.

References

[1] He YF, Wang XL, Deng SP, Wang YL, Huang QQ, Lin S, et al. Latest progress in low-intensity pulsed ultrasound for studying exosomes derived from stem progenitor cells. Front Endocrinol (Lausanne) 2023;14:1286900.
[2] Oh EJ, Lee HW, Kalimuthu S, Kim TJ, Kim HM, Baek SH, et al. In vivo migration of mesenchymal stem cells to burn injury sites and their therapeutic effects in a living mouse model. J Control Release 2018;279:79–88.
[3] Kim HK, Lee SG, Lee SW, Oh BJ, Kim JH, Kim JA, et al. A subset of paracrine factors as efficient biomarkers for predicting vascular regenerative efficacy of mesenchymal stromal/stem cells. Stem Cells 2018;37:77–88.
[4] Nakamura Y, Ishikawa H, Kawai K, Tabata Y, Suzuki S. Enhanced wound healing by topical administration of mesenchymal stem cells transfected with stromal cell-derived factor-1. Biomaterials 2013;34:9393–400.
[5] Elvasandran K, Makhoul G, Jaiswal PK, Jurakhan R, Li L, Ridwan K, et al. Tumor necrosis factor-α and hypoxia-induced secretome therapy for myocardial repair. Ann Thorac Surg 2017;105:715–23.
[6] Guo Y, Chi X, Wang Y, Heng BC, Wei Y, Zhang X, et al. Mitochondria transfer enhances proliferation, migration, and osteogenic differentiation of bone marrow mesenchymal stem cell and promotes bone defect healing. Stem Cell Res Ther 2020;11(1):245.
[7] Meng K, Cai H, Cai S, Hong Y, Zhang X. Adiponectin modified BMSCs alleviate heart fibrosis via inhibition TGF-beta1/smad in diabetic rats. Front Cell Dev Biol 2021;9:644160.
[8] Ning GZ, Song WY, Xu H, Zhu RS, Wu QL, Wu Y, et al. Bone marrow mesenchymal stem cells stimulated with low-intensity pulsed ultrasound: better choice of transplantation treatment for spinal cord injury: treatment for SCI by LIPUS-BMSCs transplantation. CNS Neurosci Ther 2019;25(4):496–508.
[9] Yang J, Chen Z, Pan D, Li H, Shen J. Umbilical cord-derived mesenchymal stem cell-derived exosomes combined pluronic F127 hydrogel promote chronic diabetic wound healing and complete skin regeneration. Int J Nanomed 2020;15:5911–26.
[10] Searle HKC, Lewis SR, Coyle C, Welch M, Griffin XL. Ultrasound and shockwave therapy for acute fractures in adults. Cochrane Database Syst Rev 2023;3(3):CD008579.
[11] Li X, Zhong Y, Zhou W, Song Y, Li W, Jin Q, et al. Low-intensity pulsed ultrasound (LIPUS) enhances the anti-inflammatory effects of bone marrow mesenchymal stem cells (BMSCs)-derived extracellular vesicles. Cell Mol Biol Lett 2023;28(1):9.
[12] Xia P, Shi Y, Wang X, Li X. Advances in the application of low-intensity pulsed ultrasound to mesenchymal stem cells. Stem Cell Res Ther 2022;13(1):214.
[13] Jiang X, Savchenko O, Li Y, Qi S, Yang T, Zhang W, et al. A Review of low-intensity pulsed ultrasound for therapeutic applications. IEEE Trans Biomed Eng 2019;66(10):2704–18.
[14] Ling L, Wei T, He L, Wang Y, Wang Y, Feng X, et al. Low-intensity pulsed ultrasound activates ERK1/2 and PI3K-Akt signalling pathways and promotes the proliferation of human amnion-derived mesenchymal stem cells. Cell Prolif 2017;50:e12383.
[15] Ruixin H, Weichen Z, Yu Z, Hu S, Yu H, Luo Y, et al. Combination of low-intensity pulsed ultrasound and C3H10T1/2 cells promotes bone-defect healing. Int Orthop 2015;39:2181–9.
[16] Chen J, Jiang J, Wang W, Qin J, Chen J, Chen W, et al. Low intensity pulsed ultrasound promotes the migration of bone marrow- derived mesenchymal stem cells via activating FAK-ERK1/2 signalling pathway. Artif Cells Nanomed Biotechnol 2019 Dec;47(1):3603–13.
[17] Liepelt A, Tacke F. Stromal cell-derived factor-1 (SDF-1) as a target in liver diseases. Am J Physiol Gastrointest Liver Physiol 2016;311(2):G203–9.
[18] Yu S, Yu S, Liu H, Liao N, Liu X. Enhancing mesenchymal stem cell survival and homing capability to improve cell engraftment efficacy for liver diseases. Stem Cell Res Ther 2023;14(1):235.
[19] Katsha AM, Ohkouchi S, Xin H, Kanehira M, Sun R, Nukiwa T, et al. Paracrine factors of multipotent stromal cells ameliorate lung injury in an elastase-induced emphysema model. Mol Ther 2011;19(1):196–203.
[20] Wakabayashi N, Sakai A, Takada H, Hoshi T, Sano H, Ichinose S, et al. Noncontact phased-array ultrasound facilitates acute wound healing in mice. Plast Reconstr Surg 2020 Feb;145(2):348e–59e.
[21] Xie S, Jiang X, Wang R, Xie S, Hua Y, Zhou S, et al. Low-intensity pulsed ultrasound promotes the proliferation of human bone mesenchymal stem cells by activating PI3K/AKt signaling pathways. J Cell Biochem 2019;120(9):15823–33.
[22] Cui JH, Park K, Park SR, Min BH. Effects of low-intensity ultrasound on chondrogenic differentiation of mesenchymal stem cells embedded in polyglycolic acid: an in vivo study. Tissue Eng 2006;12(1):75–82.
[23] Zhang S, Liu Y, Derakhshanfar S, He W, Huang Q, Dong S, et al. Polymer self-assembled BMSCs with cancer tropism and programmed homing. Adv Healthc Mater 2018;7(23):e1800118.
[24] Xia P, Wang X, Wang Q, Wang X, Lin Q, Cheng K, et al. Low-intensity pulsed ultrasound promotes autophagy-mediated migration of mesenchymal stem cells and cartilage repair. Cell Transplant 2021;30:963689720986142.
[25] Tonti GA, Mannello F. From bone marrow to therapeutic applications: different behaviour and genetic/epigenetic stability during mesenchymal stem cell expansion in autologous and foetal bovine sera? Int J Dev Biol 2008;52(8):1023–32.
[26] Bergfeld SA, DeClerck YA. Bone marrow-derived mesenchymal stem cells and the tumor microenvironment. Cancer Metastasis Rev 2010;29(2):249–61.
[27] Huang YH, Hu J, Chen F, Lecomte N, Basnet H, David CJ, et al. ID1 mediates escape from TGFβ tumor suppression in pancreatic cancer. Cancer Discov 2020;10(1):142–57.
[28] Chen DF, Zhang HL, Du SH, Li H, Zhou JH, Li YW, et al. Cholesterol myristate suppresses the apoptosis of mesenchymal stem cells via upregulation of inhibitor of differentiation. Steroids 2010;75(13–14):1119–26.
[29] Chen D, Forootan SS, Gosney JR, Forootan FS, Ke Y. Increased expression of Id1 and Id3 promotes tumorigenicity by enhancing angiogenesis and suppressing apoptosis in small cell lung cancer. Genes Cancer 2014;5:212–25.
[30] Amini A, Chien S, Bayat M. Impact of ultrasound therapy on stem cell differentiation - a systematic review. Curr Stem Cell Res Ther 2020;15(5):462–72.
[31] Lim K, Kim J, Seonwoo H, Park SH, Choung PH, Chung JH. In vitro effects of low-intensity pulsed ultrasound stimulation on the osteogenic differentiation of human alveolar bone-derived mesenchymal stem cells for tooth tissue engineering. Biomed Res Int 2013;2013:269724.
[32] Aliabouzar M, Lee SJ, Zhou X, Zhang GL, Sarkar K. Effects of scaffold microstructure and low intensity pulsed ultrasound on chondrogenic differentiation of human mesenchymal stem cells. Biotechnol Bioeng 2018;115:495–506.
[33] Zhi Z, Na T, Jue W, Zhihe Z, Lijun T. Effects of pulsed ultrasound and pulsed electromagnetic field on the extracellular matrix secretion of rat bone marrow mesenchymal stem cell pellets in chondrogenesis. Hua Xi Kou Qiang Yi Xue Za Zhi 2016;34:291–4.